Diagnostic Accuracy Study

Medicine®

OPEN

Can ultrasound elastography identify mass-like focal fatty change (FFC) from liver mass?

Tingting Qiu, MD[a], Wenwu Ling, MD[a], Jiawu Li, MD[a], Qiang Lu, MD[a], Changli Lu, MD[b], Xiaomin Li, PhD[b], Cairong Zhu, PhD[c], Yan Luo, MD[a,*]

Abstract

Focal fatty change (FFC) may mimic liver mass on conventional B-mode ultrasound. Clinical differentiation of mass-like FFC and liver mass is important due to different clinical interventions. Contrast-enhanced imaging (CEI) or biopsy is reliable for this differentiation, but is expensive and invasive. This study aimed to explore utilities of ultrasound elastography for this differentiation.

This study enrolled 79 patients with focal liver lesions (FLLs), of which 26 were mass-like FFC confirmed by at least 2 CEI modalities. The other 53 were liver masses, confirmed by pathology (n = 28) or at least 2 CEI modalities (n = 25). Lesion stiffness value (SV), absolute stiffness difference (ASD), and stiffness ratio (SR) of lesion to background were obtained using point shear-wave elastography (pSWE) and compared between FFC group and liver mass group. The performance of SV, ASD, and SR for identifying FFC from liver mass was evaluated.

SV was 5.6 ± 2.4 versus 16 ± 12 kPa, ASD was 2.0 ± 1.9 versus 11 ± 12 kPa, and SR was 1.4 ± 0.6 versus 3.0 ± 1.9 for FFC and liver mass group, respectively ($P < .0001$). The area under the receiver operating characteristic curve of SV, ASD, and SR for discriminating mass-like FFC and liver mass was 0.840, 0.842, and 0.791, respectively ($P < .05$). Particularly, with cut-off ASD < 1.0 kPa, positive predictive value was 100%, specificity was 100%, and accuracy was 82% for diagnosing FFC.

pSWE may be a potential useful modality for identifying mass-like FFC from liver mass, which might help reduce the necessity for further CEI or biopsy for diagnosing mass-like FFC.

Abbreviations: ASD = absolute stiffness difference, AUROC = area under the receiver operating characteristic curve, CECT = contrast-enhanced computer tomography, CEI = contrast-enhanced imaging, CEMRI = contrast-enhanced magnetic resonance imaging, CEUS = contrast-enhanced ultrasound, ElastPQ = Elast Point Quantification, FFC = focal fatty change, FFS = focal fat sparing, FLL = focal liver lesion, IQR/M = ratio of interquartile range to median, NPV = negative predictive value, PPV = positive predictive value, pSWE = point shear-wave elastography, SR = stiffness ratio, SV = stiffness value, SWE = shear wave elastography.

Keywords: focal fatty change, focal liver lesion, liver mass, liver stiffness measurement, ultrasound elastography

1. Introduction

Fatty liver or hepatic steatosis is a metabolic disorder of the liver where lipids accumulate in liver cells via the process of steatosis due to a variety of reasons, including obesity, diabetes, hyperlipidemia, and so on.[1] With a reported incidence of 15% to 30% on general population, fatty liver disease is becoming a prevalent health care problem worldwide.[2,3]

B-mode ultrasound is the first-line imaging tool for diagnosing fatty liver. However, on B-mode liver ultrasound, the mass-like focal fatty change (FFC) either focal fat deposition or sparing can be confused with a liver mass for their similar presentations, therefore posing a diagnostic dilemma.[4–6] Obviously, differentiation of liver mass and mass-like FFC is important in clinical practices, as different clusters need different interventions.[6] Once a liver "nodule or mass" is found on B-mode liver ultrasound, further contrast-enhanced imaging (CEI) examinations, including contrast-enhanced magnetic resonance imaging (CEMRI), contrast-enhanced computer tomography (CECT), or contrast-enhanced ultrasound (CEUS) or even biopsy, are routinely performed, which are reliable for differentiating mass-like FFC and liver mass.[7–9] However, additional costs and high requirements on experience and equipment limit its wide application, especially in developing countries.[10] Reliable and more convenient method for the discrimination of mass-like FFC and liver mass is still expected on clinic.

Very recently, technologies of shear wave based ultrasound elastography such as point shear-wave elastography (pSWE) and real-time shear wave elastography (2D-SWE) imaging have been integrated into ultrasound systems.[11] With these technologies, the stiffness of liver can be quantified in a very convenient way. The quantified liver stiffness has been proven to correlate well with the progress of liver fibrosis.[12,13] Studies using elastography to differentiate benign and malignant liver masses reported promising results, but more research is needed before it can be

Editor: Muhammed Mubarak.

Funding/support: This study was supported by National Natural Science Foundation, China (No. 81371556; 81671702; 81501488).

The authors report no conflicts of interest.

[a] Department of Ultrasound, [b] Department of Pathology, West China Hospital Sichuan University, [c] School of Public Health, Sichuan University, Chengdu, China.

[*] Correspondence: Yan Luo, Department of Ultrasound, West China Hospital Sichuan University, Chengdu 610041, China (e-mail: luoyanddoc@163.com).

Medicine (2017) 96:39(e8088)

Received: 27 April 2017 / Received in final form: 17 August 2017 / Accepted: 27 August 2017

http://dx.doi.org/10.1097/MD.0000000000008088

Table 1

Characterization of the study subjects.

Variable	Count (%)	Variable	Count (%)
Liver mass (n = 53)			
Age (y, mean ± SD)	47 ± 11	Male	35 (66)
Size (cm, mean ± SD)	5.5 ± 3.0	Pathology	28 (53)
Malignant masses (n = 25)	Benign masses (n = 28)		
HCC	14 (56)	Hemangioma	21 (75)
ICC	3 (12)	Abscess	2 (7)
Metastasis	6 (24)	FNH	5 (18)
HCC + ICC	2 (8)		
Background liver (n = 25)		Background liver (n = 28)	
Normal	0 (0)	Normal	1 (4)
Fatty	25 (100)	Fatty	27 (96)
Fibrosis/Cirrhosis	0 (0)	Fibrosis/Cirrhosis	0 (0)
Mass-like focal fatty change (n = 26)			
Age (y, mean ± SD)	46 ± 14	Male	17 (65)
Size (cm, mean ± SD)	3.2 ± 0.9	Pathology	0 (0)
Background liver (n = 26)			
Normal	13 (50)	Fibrosis/Cirrhosis	0 (0)
Fatty	13 (50)		

HCC = hepatic cell carcinoma, ICC = intrahepatic cholangiocarcinoma.

recommended in clinical practice.[12] To our knowledge, studies focusing on differentiating benign and malignant liver lesions by elastography described the stiffness of 3 to 5 cases of focal fat sparing (FFS),[14–17] but little information has been reported so far about the clinical utility of ultrasound elastography in identification of mass-like FFC from real liver mass. In our study, we tried to utilize ultrasound elastography to identify mass-like FFC from liver mass based on their possible stiffness difference.

2. Methods

2.1. Study population

This was a retrospective study adhering to Declaration of Helsinki for Medical Research involving Human Subjects and it was approved by the ethics committee of West China Hospital, Sichuan University. Written informed consents were obtained from all patients. From July 2015 to July 2016, 101 patients with grey-scale ultrasound demonstrated hyperechoic "nodule or mass" on a normal liver background or hypoechoic "nodule or mass" on a hyperechoic liver background, but no signs of significant liver fibrosis or cirrhosis were consecutively enrolled in this study. "Nodule or mass" referred to focal liver lesion, which presented as "nodule or mass" for at least 2 different scanning planes on B-mode image. For patients with multiple lesions, the largest one was chosen as the study subject. Exclusion criteria include patients who failed in pSWE examination due to the small size of lesion (<1 cm, n = 5), deep location of lesion (>7 cm from transducer, n = 3), or excessive respiratory movement during examination (n = 3); patients with a focal liver lesion; however, neither pathology nor CEI modalities were performed for the confirmation of diagnosis (n = 11).

Characteristics of the study participants are presented in Table 1. Finally, 79 patients were studied, including 53 patients with liver masses diagnosed by pathology (n = 28) or CEI modalities (n = 25) and 26 patients with mass-like FFCs diagnosed by CEI modalities. Of the 53 liver masses, 25 (47%) were benign masses and 28 (53%) were malignant masses. Fifty-two patients (98%) had simple fatty[18] liver background and 1 (2%) had normal liver background. Of the 26 mass-like FFCs, 13 (50%) had normal liver background and 13 (50%) had simple fatty[18] liver background.

2.2. B-mode ultrasound examination

All patients received B-mode liver ultrasound scanning before pSWE examination. The scanning and diagnosis were conducted by 1 experienced (>5 years) ultrasound doctor who was blinded to the final diagnosis of the FLL. An iU22 ultrasound system (Royal Philips, the Netherlands) equipped with C5–1 (1–5 MHz) transducer was applied for the examinations. The settings [gain, depth, contrast, and mechanical index (MI)] were optimized for each patient.

2.3. pSWE examination

pSWE measurements were performed using the same ultrasound system after B-mode examination by the same ultrasound doctor (>3 years of experience on ElastPQ examination). The size for measurement region of interest (ROI) of ElastPQ was depth dependent with 0.5 cm × 1.5 cm at the depth of 4 cm. The average depth of the measurements was about 4.0 cm, range 3 to 7 cm.[12] The quantified tissue stiffness was expressed in kilopascals (kPa) and displayed over a B-mode ultrasound image (Fig. 1).

For each patient, 10 ElastPQ measurements were performed on the lesion and background liver (at ≥2 cm away from lesion periphery), respectively, at the similar depth.[19] The IQR/M (ratio of interquartile range to median) < 30% was considered as successful measurement.[13] The measurement was taken during a 5-second breath-hold at the same breathing phase for

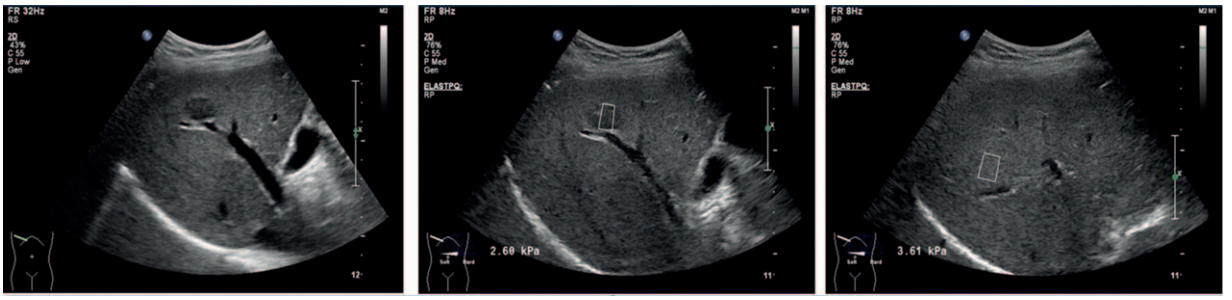

Figure 1. In vivo stiffness measurements of 26 patients with mass-like focal fatty changes (FFCs). Stiffness measurement of a mass-like focal fatty change and its fatty background liver displayed over B-mode ultrasound images. The white boxes represent regions of interest for stiffness measurement.

each patient.[20] Lesion stiffness value (SV), absolute stiffness difference (ASD), and stiffness ratio (SR) of lesion to background were calculated and compared between FFC group and liver mass group. Furthermore, the diagnostic performance of SV, ASD, and SR in the differentiation of liver mass and mass-like FFC was investigated.

2.4. CEUS, CEMRI, CECT examinations

CEI was performed after B-mode and pSWE examination. Diagnosis was made independently by 2 ultrasound doctors who were blinded to the pSWE results, each with more than 10 years of experience in CEUS. The final diagnosis was the consensus of the 2 ultrasound doctors. CEUS examination was performed with the same ultrasound machine. MI was set at 0.05. Ultrasound contrast agent of 1.2 mL SonoVue (Bracco, Milan, Italy) was injected into the cubital vein of each patient. CEMRI examination was performed using a 1.5-T MR unit (Siemens Medical Solutions, Erlangen, Germany) with a high pressure syringe injection (injection rate was 2–3 mL/s) of 0.2 mmol/kg gadopentetatedimeglumine contrast agent (Magnevist, Bayer Schering Pharma AG) through median cubital vein. CECT examination was performed by a 64-channel multi-slice computed tomographic (CT) scanner (Royal Philips, the Netherlands) with a high pressure syringe injection (injection rate was 3 mL/s) of 80 to 100 mL iodinated contrast material Ultravist (Bayer Schering Pharma, Berlin-Wedding, Germany) through median cubital vein.

The enhancement pattern of a lesion during arterial phase, portal phase, and delay phase was evaluated with the surrounding parenchyma as reference. FFC showed exactly the same enhancement patterns as the surrounding parenchyma in all phases, while other liver masses presented a different enhancement pattern from the reference in any phase.[7–9]

2.5. Pathological examination

Surgical specimens of liver lesions were fixed with 10% formalin, and routinely embedded in paraffin. The tissue sections were stained with hematoxylin and eosin (H&E). Pathological diagnosis was independently performed by 2 pathologists, each with more than 7 years of experience. The final diagnosis was the consensus of the 2 pathologists.

2.6. Statistical analysis

Three stiffness parameters, SV, ASD, and SR, were calculated for each individual. Box-and-whisker plot was employed on the original data to display the data distribution. Mann–Whitney unpaired test was performed on the log2 transformed data to determine the significance of difference between 2 variables. All the P values were 2-sided. The difference was considered significant if P value was smaller than .05. Capabilities of lesion SV, ASD, and SR in the differentiation of mass-like FFC and liver mass were analyzed via receiver operating characteristic (ROC) curve analysis. The area under the ROC curve (AUROC), accuracy, sensitivity, specificity, positive prediction value (PPV), and negative prediction value (NPV) were calculated. Accuracy, sensitivity, specificity, PPV, and NPV were calculated with the optimal cut-offs that maximized the PPV for diagnosing FFC. MedCalc (10.4.7.0, Ostend, Belgium) Software was used to perform statistical analysis.

3. Results

3.1. Stiffness measurements on mass-like FFC, liver mass, and background liver

The distributions of SV on mass-like FFCs, liver masses, and background liver are illustrated in Fig. 2 and Table 2. Significantly higher SV was found on liver masses than mass-like FFCs (16 ± 12 vs 5.6 ± 2.4 kPa, $P < .0001$). The background liver stiffness of mass-like FFC group and liver mass group was 4.1 ± 1.4 and 4.9 ± 1.6 kPa, respectively ($P = .0131$).

3.2. Absolute stiffness difference and stiffness ratio between liver mass and mass-like FFC

Profiles for ASD and SR are illustrated in Fig. 3 and Table 2. The mean ASD was 2.0 ± 1.9 kPa (range 0.06–6.0 kPa) for the mass-like FFC group, while the mean ASD for the liver mass group was 11 ± 12 kPa (range 1.0–58 kPa), as illustrated in Fig. 3A. Mean ASD of the liver mass group was significantly higher than the mass-like FFC group ($P < .0001$, Table 2).

As illustrated in Fig. 3B, the mean SR was 1.4 ± 0.6 (range 0.5–2.9) and 3.0 ± 1.9 (range 0.6–7.5), respectively, for the mass-like FFC group and liver mass group. SR of mass-like FFC group was significantly lower than that of the liver mass group ($P < .0001$).

3.3. Capabilities of lesion SV, ASD, SR in the differentiation of liver mass and mass-like FFC

Diagnostic performance of SV, ASD, and SR for the differentiation of mass-like FFC and liver mass is presented in Fig. 4 and Table 3. The AUROC was 0.840 (0.740–0.913), 0.842 (0.742–0.915), and 0.791 (0.685–0.875) for SV, ASD, and SR, respectively. No significantly different AUROCs were found among the 3 parameters (ASD vs SV $P = .942$; ASD vs SR $P = .101$; SV vs SR $P = .149$) as illustrated in Fig. 4.

As revealed in Table 3, with the optimal cut-off lesion SV < 5.2 kPa, the PPV, accuracy, sensitivity, specificity, and NPV for diagnosing FFC was 76%, 78%, 50%, 92%, and 79%, respectively. With the cut-off ASD < 1.0 kPa, the PPV, accuracy, sensitivity, specificity, and NPV for diagnosing FFC was 100%, 82%, 46%, 100%, and 79%, respectively. With the cut-off SR $<$ 0.6, the PPV, accuracy, sensitivity, specificity, and NPV for diagnosing FFC was 100%, 68%, 8%, 100%, and 69%, respectively.

4. Discussion

With a change in lifestyle, fatty liver is becoming an important health concern worldwide. Not only in Western countries, the incidence of fatty liver also rises dramatically in developing countries.[21] Fatty liver can be homogeneous or heterogeneous. The heterogeneous fatty liver, especially mass-like FFC, is very likely misdiagnosed as hemangiomas, metastases, hepatic cell carcinoma, or other liver masses on B-mode ultrasound.[4,5,22] The differentiation of mass-like FFC and real liver mass is vital in clinical practices, as different interventions would be applied. For patients with FFC, change in lifestyle and investigation on the underlying conditions are required to prevent the further progress of disease,[3] while for patients with a liver mass, follow-ups, medications, surgeries, and other therapies are required depending on the nature of the liver mass. Although CEI modalities or

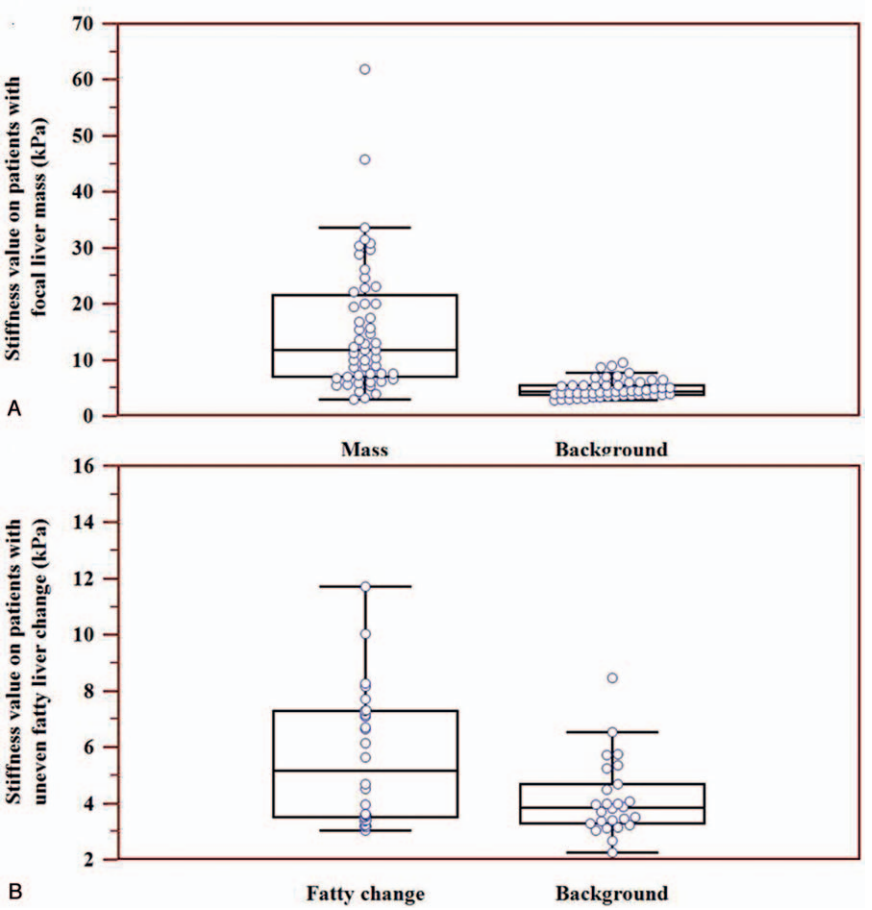

Figure 2. (A) Box-and-whisker plot of in vivo stiffness values of 53 liver masses and their background (normal, fatty). (B) Box-and-whisker plot of in vivo SV (stiffness values) of 26 mass-like focal fatty changes and their background (normal, fatty). Means of 5 measurements within an individual were used in the plot.

biopsy have a more definite answer to this differentiation, they require higher costs and are not widely available. More convenient and efficient means for identifying FFC from liver mass may help reduce the necessity for further CEI or other examinations for FFC.

Ultrasound elastography has been considered as a useful tool for liver fibrosis assessment.[12,13] For differentiating benign and malignant focal liver lesions by ultrasound elastography, study results were promising,[14,23,24] but more research is needed for its clinical recommendation.[12] As for the differentiation of mass-like FFC and liver mass using ultrasound elastography, related information was quite limited to our knowledge. Therefore, instead of discriminating benign from malignant, our study focused on investigating the utility of ultrasound elastography for identifying mass-like FFC from liver mass, which was different from previous studies. Furthermore, we used 3 stiffness parameters (SV, ASD, SR) simultaneously to evaluate the difference of stiffness between mass-like FFC and liver mass group, which were more than the stiffness parameters used in most previous studies.

In our study by ElastPQ, the mean SV on 26 mass-like FFCs was 5.6 ± 2.4 kPa. It was significantly lower than that of the 53 liver masses (16 ± 12 kPa, $P < .0001$). The different SV of mass-like FFC and liver mass could be explained by their difference in pathology. Most of liver masses are composed of hyperplastic or irregular hepatic cells with fibrous septa or increased abnormal vessel structure.[25–27] However, mass-like FFC is induced by the inhomogeneous accumulation of intracellular fat within hepatic parenchyma due to altered blood supply and insulin level.[28–30] The SV of FFS has been mentioned by Guibal et al,[14] Heide

Table 2

Stiffness profiles on mass-like focal fatty change and liver mass.

Variables	Lesion stiffness (kPa, mean ± SD, range)	Background stiffness (kPa, mean ± SD, range)	Stiffness difference (kPa, mean ± SD, range)	Stiffness ratio (mean ± SD, range)
Liver mass	16 ± 12 (3.0–62)	4.9 ± 1.6 (2.8–9.6)	11 ± 12 (1.0–58)	3.0 ± 1.9 (0.6–7.5)
Focal fatty change	5.6 ± 2.4 (3.0–12)	4.1 ± 1.4 (2.2–8.5)	2.0 ± 1.9 (0.06–6.0)	1.4 ± 0.6 (0.5–2.9)
Folder change	0.4	0.8	0.2	0.5
P	<.0001	.0131	<.0001	<.0001

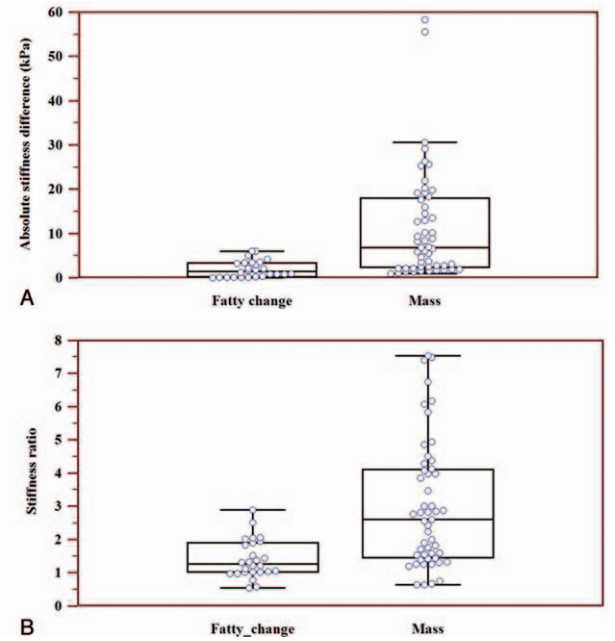

Figure 3. (A) Box-and-whisker plot of in vivo ASD (absolute stiffness difference of lesion and background liver) of 26 mass-like focal fatty changes and 53 liver masses. (B) Box-and-whisker plot of in vivo SR (stiffness ratio of lesion to background liver) of 26 mass-like focal fatty changes and 53 liver masses.

et al,[15] and Ronot et al,[16] in their study. In the study by Guibal et al[14] by SWE, the mean SV on 3 FFS was 6.6 ± 0.3 kPa. In the study by Heide et al[15] by ARFI, the shear wave velocity was measured on 3 FFS and the mean shear wave velocity was 1.02 ± 1.16 m/s (around 3.1 ± 4.0 kPa). Those results were close to ours (5.6 ± 2.4 kPa). While in Ronot's study by SWE, the mean SV on 5 FFS was 11.3 ± 4.3 kPa.[16] We further studied SR on patients with mass-like FFC and on patients with liver mass. Significantly higher SR (3.0 ± 1.9 vs 1.4 ± 0.6, $P < .0001$) was observed on patients with liver mass than patients with mass-like FFC. In Ronot's study by SWE, the SR of FFS was 1.5 ± 0.62, which was quite similar to our consequence (1.4 ± 0.6).[16] However, in the

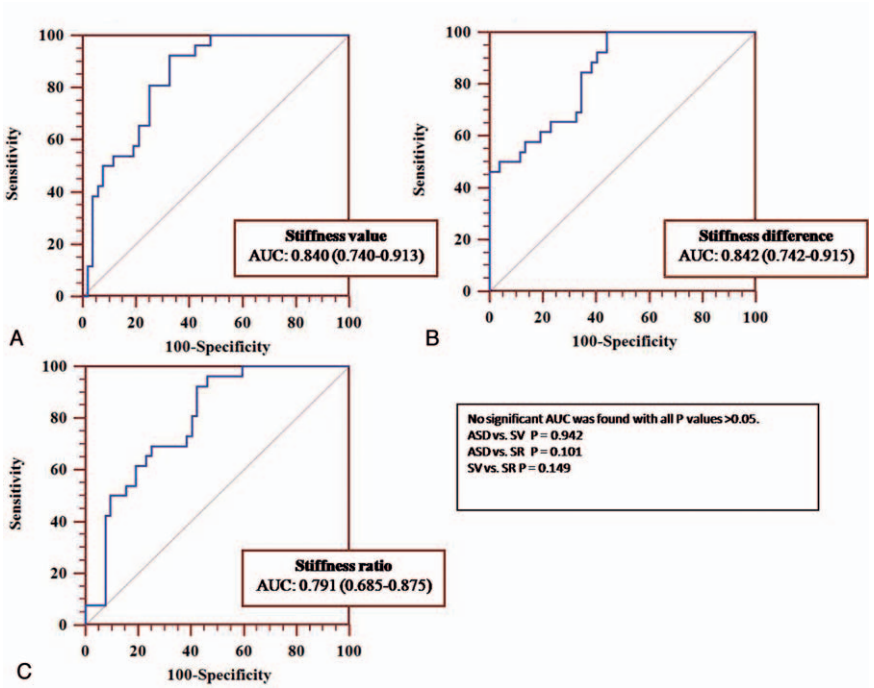

Figure 4. (A) Receiver operating characteristic (ROC) curve of stiffness value. Area under the curve (AUC) was 0.840. (B) ROC curve of absolute stiffness difference and the AUC was 0.842. (C) ROC curve of stiffness ratio and the AUC was 0.791.

Table 3

Comparison on diagnostic performance of stiffness value, stiffness difference, and stiffness ratio.

Variables	AUC (95% CI)	Cut-off	Focal fatty change (n = 26)	Liver mass (n = 53)	Accuracy	Sensitivity	Specificity	PPV	NPV
Stiffness value	0.840 (0.740–0.913)	<5.2 kPa	13	4	82%	50%	92%	76%	79%
Stiffness difference	0.842 (0.742–0.915)	<1.0 kPa	12	0	82%	46%	100%	100%	79%
			14	53					
Stiffness ratio	0.791 (0.685–0.875)	<0.6	2	0	68%	8%	100%	100%	69%
			24	53					

Cut-off was calculated to maximize the PPV for detecting FFC.

95% CI = 95% confidence interval, AUC = area under the curve, NPV = negative predictive value, PPV = positive predictive value.

study by Park et al, [17] the SR of FFS was 2.3 ± 0.77. The inconsistent SV and SR on FFS across different studies might be induced by the different technologies utilized and the limited number of study subjects would also influence the statistic results. In this study, ASD of mass-like FFC was significantly lower than liver mass (2.0 ± 1.9 vs 11 ± 12 kPa, $P < .0001$). Through literature review, published data using ASD to characterize FFC by ultrasound elastography has not been searched yet. Other imaging method such as diffusion-weighted MRI (DWI) revealed that steatosis significantly decreased ADC (apparent diffusion coefficient) value in patients with HCV-related early and advanced stages of liver fibrosis.[31] DWI indicated the structural difference quantitatively between steatosis and fibrosis, which was similar to the result of this study.

For the diagnostic performance of SV, ASD, and SR on differentiating mass-like FFC and liver mass, this study illustrated comparable capabilities of SV, ASD, and SR with AUROCs of 0.840, 0.842, and 0.791, respectively. When mass-like FFC is confused with liver mass, the clinical or radiological expectation is to identify FFC from real liver mass first and then adopt further examinations to confirm the nature of liver mass.[6] Therefore, we identified the cut-off value that corresponds to the maximal PPV value for diagnosing FFC and then calculated the accuracy, sensitivity, specificity, and NPV. As illustrated in Table 3, both ASD and SR illustrated PPV of 100% when the cut-off value was set to maximize the PPV for detecting FFC. However, ASD had significantly higher sensitivity and accuracy than SR (sensitivity: 46% vs 8%; accuracy: 82% vs 68%). With cut-off ASD < 1.0 kPa, the accuracy, sensitivity, and specificity was 82% (65/79), 46% (12/26), and 100% (12/12), respectively, for diagnosing FFC. The result indicated that if the ASD of a suspicious "mass" was lower than 1 kPa, the lesion had very high probability to be FFC and could be triaged from liver mass. Therefore, further CEI or other examinations might be avoided.

Considering the easier clinical feasibility and fast and economic characteristics of ultrasound elastography, we tried to identify mass-like FFC from liver mass based on their stiffness difference. Although the result needs further validation, it is promising that ultrasound elastography may be useful for primary triage of mass-like FFC from liver mass, which might avoid further CEI or other examinations for diagnosing FFC. However, we still have some limitations. First, selection bias existed since only patients with simple fatty or normal liver background were enrolled in this preliminary study. Studies including various liver backgrounds on larger cohorts of subjects should be performed in the following study. Limited by the size of measurement ROI of ElastPQ, all lesions analyzed in this study were larger than 1 cm. Studies on smaller lesions (≤1 cm) should be conducted. Meanwhile, further studies using different elastography technologies for this differentiation may need to be compared.

In conclusion, pSWE may be a potential useful modality for identifying mass-like FFC from liver mass, which might help reduce the necessity for further CEI or biopsy for diagnosing mass-like FFC.

References

[1] Yeh MM, Brunt EM. Pathological features of fatty liver disease. Gastroenterology 2014;147:754–64.

[2] Younossi ZM, Koenig AB, Abdelatif D, et al. Global epidemiology of nonalcoholic fatty liver disease: meta-analytic assessment of prevalence, incidence, and outcomes. Hepatology 2016;64:73–84.

[3] Gao X, Fan J-G. Diagnosis and management of non-alcoholic fatty liver disease and related metabolic disorders: consensus statement from the Study Group of Liver and Metabolism, Chinese Society of Endocrinology. J Diabetes 2013;5:406–15.

[4] Dong BW, Chen MH, Li JG, et al. Further study on sonographic patterns of non-formity fatty liver. Chinese J Ultrasonogr 1993;2:62–3.

[5] Wang SS1 , Chiang JH, Tsai YT, et al. Focal hepatic fatty infiltration as a cause of pseudotumors: ultrasonographic patterns and clinical differentiation. J Clin Ultrasound 1990;18:401–9.

[6] Bhatnagar G, Sidhu HS, Vardhanabhuti V, et al. The varied sonographic appearances of focal fatty liver disease: review and diagnostic algorithm. Clin Radiol 2012;67:372–9.

[7] Claudon M, Dietrich CF, Choi BI, et al. Guidelines and good clinical practice recommendations for contrast enhanced ultrasound (CEUS) in the liver: update 2012: a WFUMB-EFSUMB initiative in cooperation with representatives of AFSUMB, AIUM, ASUM, FLAUS ICUS. Ultrasound Med Biol 2012;39:187–210.

[8] Onishi H, Theisen D, Dietrich O, et al. Hepatic steatosis: effect on hepatocyte enhancement with gadoxetate disodium-enhanced liver MR imaging. J Magn Reson Imaging 2014;39:42–50.

[9] Lawrence DA, Oliva IB, Israel GM. Detection of hepatic steatosis on contrast-enhanced CT images: diagnostic accuracy of identification of areas of presumed focal fatty sparing. Am J Roentgenol 2012;199:44–7.

[10] Dietrich CF, Ignee A, Hocke M, et al. Pitfalls and artefacts using contrast enhanced ultrasound. Z Gastroenterol 2011;49:350–6.

[11] Bamber J, Cosgrove D, Dietrich CF, et al. EFSUMB guidelines and recommendations on the clinical use of ultrasound elastography. Part 1: basic principles and technology. Ultraschall Med 2013;34:169–84.

[12] Cosgrove D, Piscaglia F, Bamber J, et al. EFSUMB guidelines and recommendations on the clinical use of ultrasound elastography. Part 2: clinical applications. Ultraschall Med 2013;34:238–53.

[13] Latinoamericana A. EASL-ALEH Clinical Practice Guidelines: non-invasive tests for evaluation of liver disease severity and prognosis. J Hepatol 2015;63:237–64.

[14] Guibal A, Boularan C, Bruce M, et al. Evaluation of shearwave elastography for the characterisation of focal liver lesions on ultrasound. Eur Radiol 2013;23:1138–49.

[15] Heide R, Strobel D, Bernatik T, et al. Characterization of focal liver lesions (FLL) with acoustic radiation force impulse (ARFI) elastometry. Ultraschall Med 2010;31:405–9.

[16] Ronot M, Di Renzo S, Gregoli B, et al. Characterization of fortuitously discovered focal liver lesions: additional information provided by shearwave elastography. Eur Radiol 2014;25:346–58.

[17] Park HS, Kim YJ, Yu MH, et al. Shear wave elastography of focal liver lesion: intraobserver reproducibility and elasticity characterization. Ultrasound Q 2015;31:262–71.
[18] European Association for the Study of the Liver (EASL); European Association for the Study of Diabetes (EASD); European Association for the Study of Obesity (EASO)European Association for the Study of the Liver (EASL); European Association for the Study of Diabetes (EASD); European Association for the Study of Obesity (EASO)EASL-EASD-EASO Clinical Practice Guidelines for the management of non-alcoholic fatty liver disease. J Hepatol 2016;64:1388–402.
[19] Park H, Park JY, Kim DY, et al. Characterization of focal liver masses using acoustic radiation force impulse elastography. World J Gastroenterol 2013;19:219–26.
[20] Ling W, Lu Q, Quan J, et al. Assessment of impact factors on shear wave based liver stiffness measurement. Eur J Radiol 2013;82:335–41.
[21] Blais P, Husain N, Kramer JR, et al. Nonalcoholic fatty liver disease is underrecognized in the primary care setting. Am J Gastroenterol 2015;110:10–4.
[22] Karcaaltincaba M, Akhan O. Imaging of hepatic steatosis and fatty sparing. Eur J Radiol 2007;61:33–43.
[23] Ying L, Lin X, Xie Z-L, et al. Clinical utility of acoustic radiation force impulse imaging for identification of malignant liver lesions: a meta-analysis. Eur Radiol 2012;22:2798–805.
[24] Yu H, Wilson SR. Differentiation of benign from malignant liver masses with Acoustic Radiation Force Impulse technique. Ultrasound Q 2011;27:217–23.
[25] Laumonier H, Bioulac-Sage P, Laurent C, et al. Hepatocellular adenomas: magnetic resonance imaging features as a function of molecular pathological classification. Hepatology 2008;48:808–18.
[26] Gallotti A, D'Onofrio M, Romanini L, et al. Acoustic Radiation Force Impulse (ARFI) ultrasound imaging of solid focal liver lesions. Eur J Radiol 2012;81:451–5.
[27] Frulio N, Laumonier H, Carteret T, et al. Evaluation of liver tumors using acoustic radiation force impulse elastography and correlation with histologic data. J Ultrasound Med 2013;32:121–30.
[28] Fukukura Y, Fujiyoshi F, Inoue H, et al. Focal fatty infiltration in the posterior aspect of hepatic segment IV: relationship to pancreaticoduodenal venous drainage. Am J Gastroenterol 2000;95:3590–5.
[29] Vilgrain V, Ronot M, Abdel-Rehim M, et al. Hepatic steatosis: a major trap in liver imaging. Diagn Interv Imaging 2013;94:713–27.
[30] Unal E, Ozmen MN, Akata D, et al. Imaging of aberrant left gastric vein and associated pseudolesions of segments II and III of the liver and mimickers. Diagnostic Interv Radiol 2015;21:105–10.
[31] Besheer T1, Razek AAKA, El Bendary M, et al. Does steatosis affect the performance of diffusion-weighted MRI values for fibrosis evaluation in patients with chronic hepatitis C genotype 4? Turk J Gastroenterol 2017;28:283–8.